the eastern coast of the Antarctic Peninsula. Not surprisingly, the scientific community is currently devoting considerable energy to attempting to answer these questions. One could say that a cold subject is heating up.

See also

Antarctic Circumpolar Current. Arctic Basin Circulation. Icebergs. Sea Ice: Variations in Extent and Thickness.

Further Reading

Cavelieri DJ, Gloersen P, Parkinson CL, Comiso JC and Zwally HJ (1997) Observed hemispheric asymmetry in global sea ice changes. *Science* 278(5340): 1104–1106.

Dyer I and Chryssostomidis C (eds) (1993) *Arctic Technology and Policy*. New York: Hemisphere.

Leppäranta M (ed.) (1998) *Physics of Ice-covered Seas*, 2 vols. Helsinki. Helsinki University Printing House.

McLaren AS (1989) The underice thickness distribution of the Arctic basin as recorded in 1958 and 1970. *Journal of Geophysical Research* 94(C4): 4971–4983.

Morison JH, Aagaard K and Steele M (1998) *Study of the Arctic Change Workshop*. (Report on the Study of the Arctic Change Workshop held 10–12 November 1997, University of Washington, Seattle, WA). Arctic System Science Ocean–Atmosphere–Ice Interactions Report No. 8 (August 1998).

Rothrock DA, Yu Y and Maykut G (1999) Thinning of the Arctic sea ice cover. *Geophysical Research Letters* 26.

Untersteiner N (ed.) (1986) *The Geophysics of Sea Ice*. NATO Advanced Science Institutes Series B, Physics, vol. 146. New York: Plenum Press.

Variations in Extent and Thickness

P. Wadhams, University of Cambridge, Cambridge, UK

doi:10.1006/rwos.2001.0004

This review considers the seasonal and interannual variability of sea ice extent and thickness in the Arctic and Antarctic, and the downward trends which have recently been shown to exist in Arctic thickness and extent. There is no evidence at present for any thinning or retreat of the Antarctic sea ice cover.

Sea Ice Extent

Arctic

Seasonal variability The best way of surveying sea ice extent and its variability is by the use of satellite imagery, and the most useful imagery on the large scale is passive microwave, which identifies types of surface through their natural microwave emissions, a function of surface temperature and emissivity. **Figure 1** shows ice extent and concentration maps for the Arctic for each month, averaged over the period 1979–87, derived from the multifrequency SMMR (scanning multichannel microwave radiometer) sensor aboard the Nimbus-7 satellite. This instrument gives ice concentration and, through comparison of emissions at different frequencies, the percentage of the ice cover that is multiyear ice, i.e. ice which has survived at least one summer of melt. The ice concentrations are estimated to be accurate to $\pm 7\%$.

At the time of maximum advance, in February and March (**Figure 1A**), an ice cover fills the entire Arctic Ocean. The Siberian shelf seas are also ice-covered to the coast, although the warm inflow from the Norwegian Atlantic Current keeps the western part of the Barents Sea open. There is also a bight of open water to the west of Svalbard, kept open by the warm West Spitsbergen Current and formerly known as Whalers' Bay because it allowed sailing whalers to reach high latitudes. It is here that open sea is found closest to the Pole in winter – beyond 81° in some years. The east coast of Greenland has a sea ice cover along its entire length (although in mild winters the ice fails to reach Cape Farewell); this is transported out of Fram Strait by the Trans Polar Drift Stream and advected southward in the East Greenland Current, the strongest part of the current (and so the fastest ice drift) being concentrated at the shelf break. The Odden ice tongue at 72–75°N can be seen in these averaged maps as a distinct bulge in the ice edge, visible from January until April with an ice concentration of 20–50%. During any given year the Odden feature usually develops in the shape of a tongue, covering the region influenced by the Jan Mayen Current (a cold eastward offshoot of the East Greenland Current) and composed mainly of locally formed pancake ice.

Moving round Cape Farewell there is a thin band of ice off West Greenland (called the 'Storis'), the

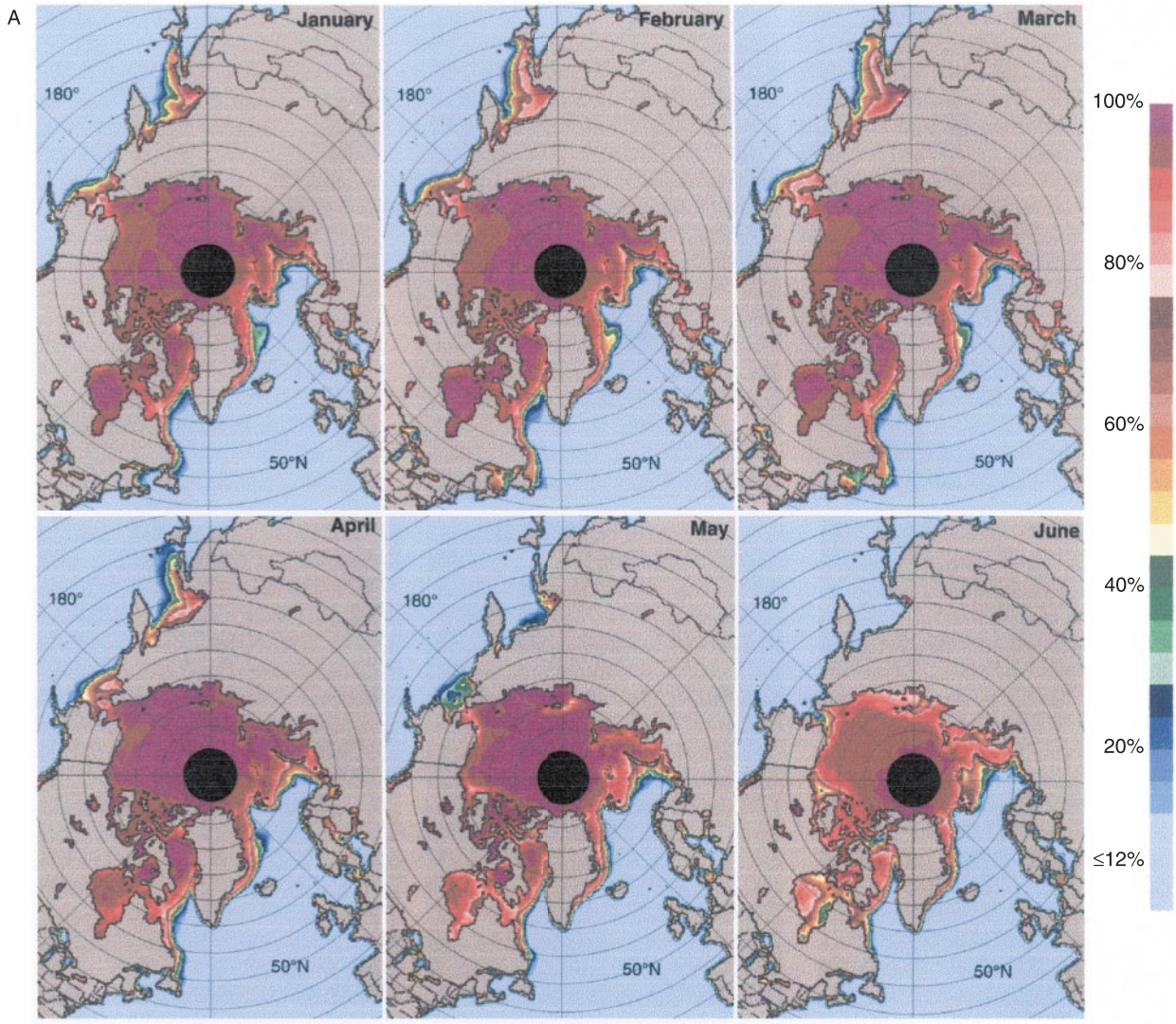

Figure 1 Ice extent and concentration maps for the Arctic for (A) winter, (B) summer months, averaged over the period 1979–87, derived from the multifrequency SMMR sensor aboard the Nimbus 7 satellite. (Reproduced with permission from Gloersen *et al.*, 1992.)

limit of ice transported out of the Arctic Basin, which often merges with the dense locally formed ice cover of Baffin Bay and Davis Strait. The whole of the Canadian Arctic Archipelago, Hudson Bay, and Hudson Strait are ice-covered, and on the western side of Davis Strait the ice stream of the Labrador Current carries ice out of Baffin Bay southward towards Newfoundland. The southernmost ice limit of this drift stream is usually the north coast of Newfoundland, where the ice is separated by the bulk of the island from an independently formed ice cover filling the Gulf of St Lawrence, with the ice-filled St Lawrence River and Great Lakes behind. Further to the west a complete ice cover extends across the Arctic coasts of north-west Canada and Alaska and fills the Bering Sea, at somewhat lower concentration, as far as the shelf break. Sea ice also fills the Sea of Okhotsk and the northern end of the Sea of Japan, with the north coast of Hokkaido experiencing the lowest latitude sea ice (44°) in the Northern Hemisphere.

In April the ice begins to retreat from its low latitude extremes. By May the Gulf of St Lawrence is clear, as is most of the Sea of Okhotsk and some of the Bering Sea. The Odden ice tongue has disappeared and the ice edge is retreating up the east coast of Greenland. By June the Pacific south of Bering Strait is ice-free, with the ice concentration reducing in Hudson Bay and several Arctic coastal locations. August and September (**Figure 1B**) are the

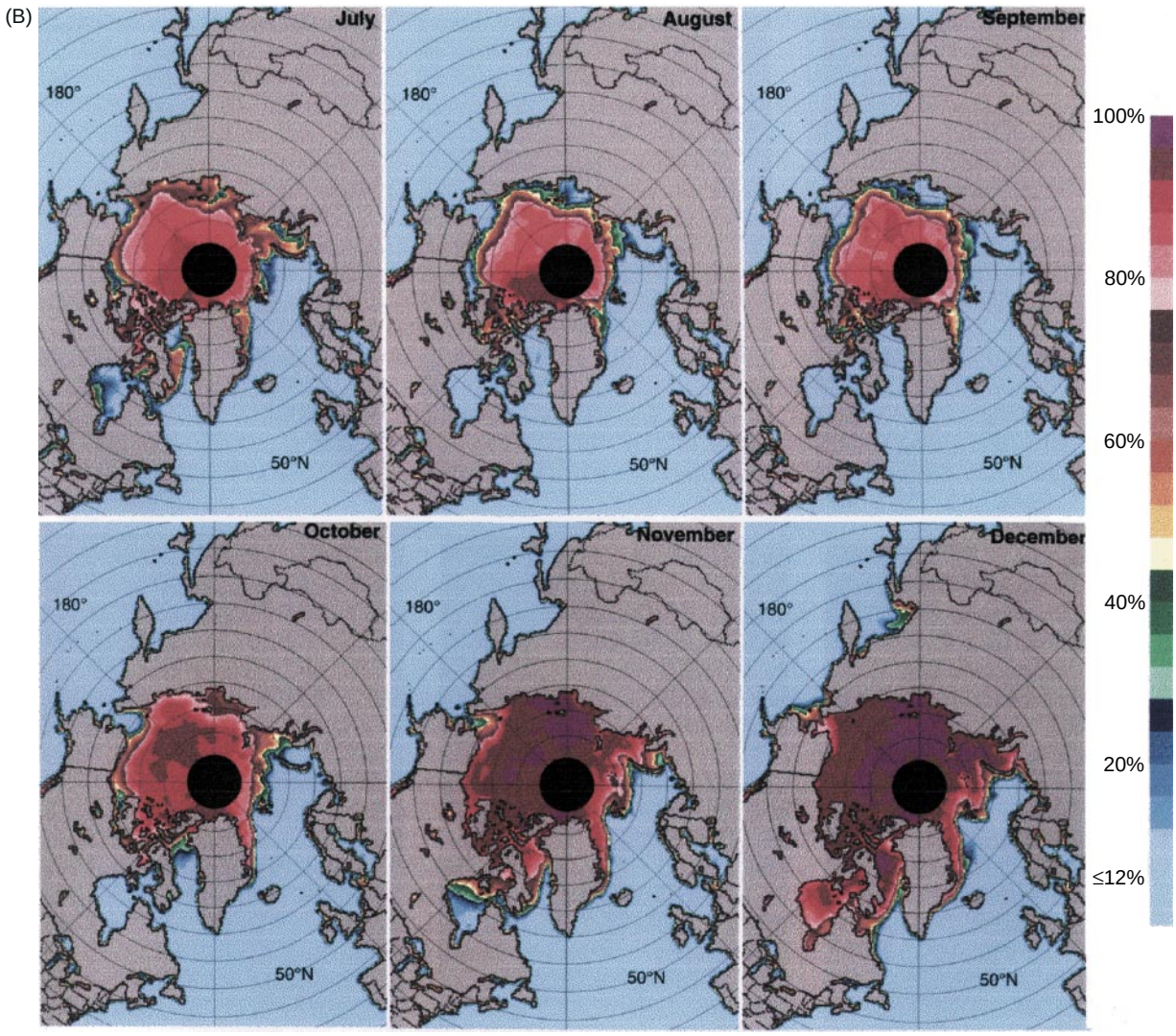

Figure 1 *Continued*

months of greatest retreat, constituting the brief Arctic summer. During these months the Barents and Kara Seas are ice-free as far as the shelf break, with the Arctic pack retreating to (and occasionally beyond) northern Svalbard and Franz Josef Land. The Laptev and East Siberian Sea are generally ice-free, with ice in some years remaining to block choke points such as the Vilkitsky Strait south of Severnaya Zemlya. This allows marine transport through a Northern Sea Route across the top of Russia, but with a need for icebreaker escort through the central ice-choked region. In East Greenland the ice has retreated northwards to about 72–73° (a latitude which varies greatly from year to year), while the whole system of Baffin Bay, Hudson Bay, and Labrador is ice-free. Occasionally a small mass of ice, called the 'Middle Ice', remains at the northern end of Baffin Bay. In the Canadian Arctic Archipelago the winter fast ice which filled the channels usually breaks up and partly melts or moves out, but in some years ice remains to clog vital channels, and the Northwest Passage is not such a dependably navigable seaway as the Northern Sea Route. There is usually a slot of open water across the north of Alaska, but again in some years the main Arctic ice edge moves south to touch the Alaskan coast, making navigation very difficult for anything but a full icebreaker.

By October new ice has formed in many of the areas which were open in summer, especially around the Arctic Ocean coasts, and in November–January there is steady advance everywhere towards the winter peak. The Sea of Okhotsk acquires its first ice cover in December, and the Odden starts

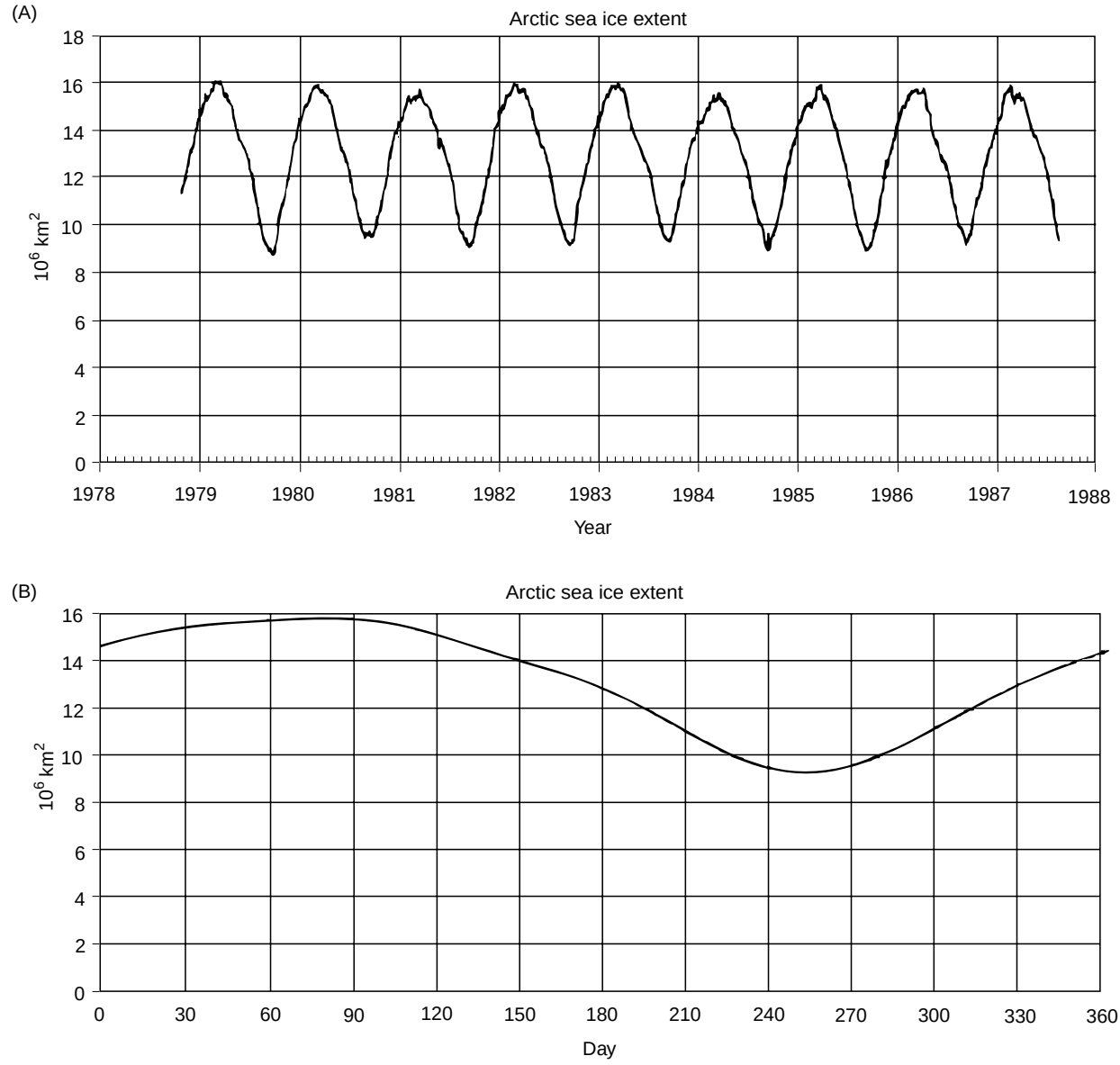

Figure 2 (A) The cycle of Arctic sea ice extent for the 1979–87 period; (B) the averaged seasonal cycle. (Reproduced with permission from Gloersen *et al.*, 1992.).

to appear; Baffin Bay and Hudson Bay are already fully ice-covered.

The averaged seasonal cycle for the 1979–87 era (**Figure 2B**) gives a maximum extent – 'extent' here is defined as the total area of sea within the 15% ice concentration contour – of $15.7 \times 10^6\,\text{km}^2$ in late March, and a minimum of $9.3 \times 10^6\,\text{km}^2$ in early September. For sea ice area, derived as extent multiplied by concentration, the figures are 13.9 and $6.2 \times 10^6\,\text{km}^2$ in winter and summer.

Results from SMMR multiyear ice retrievals show that in the Arctic multiyear ice is found in the highest concentrations within the central Arctic Ocean, in the area controlled by the Beaufort Gyre. This is not surprising, since the area is permanently ice-covered and floes circulate on closed paths which take 7–10 years for a complete circuit. It was found that multiyear fractions of 50–60% are typical for the Gyre region, rising to 80% in the very centre. Multiyear fractions of 30–40% are found in the part of the Trans Polar Drift Stream fringing the Beaufort Gyre, while in the rest of this current and in peripheral areas of the Arctic the multi–year fraction is $\leqslant 20\%$.

Interannual variability The seasonal cycle described above varies in detail from year to year, and there is evidence from an extension of the record to

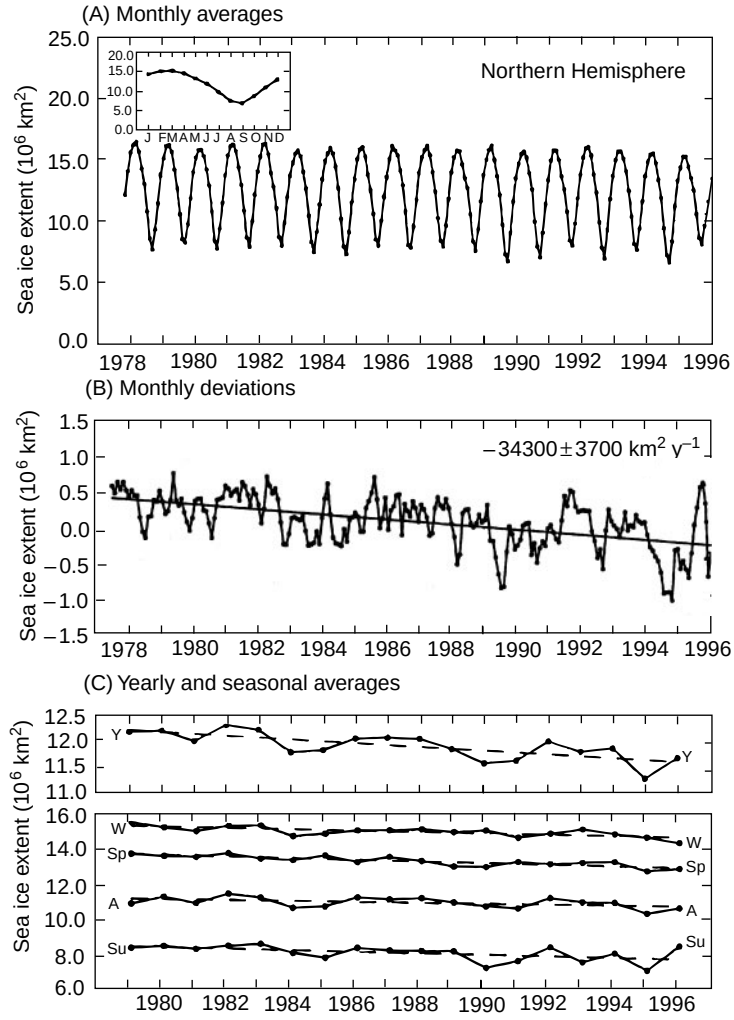

Figure 3 (A) Monthly averaged Northern Hemisphere sea ice extents from SMMR and SSM/I data, November 1978–December 1996. Inset shows average seasonal cycle. (B) Monthly deviations of the extents from the 18-year average, with linear trend shown. (C) Yearly and seasonally averaged ice extents: W = January–March, Sp = April–June, Su = July–September, A = October–December. (Reproduced with permission from Parkinson *et al.* (1999) *Journal of Geophysical Research,* 104: 20837–20856.

the present day that a steady decrease of the overall ice extent in the Arctic has been taking place. Analyses where datasets from the SMMR and newer SSM/I sensors have been combined and reconciled show that the sea ice extent in the Arctic has declined at a decadal rate of some 2.8–3% since 1978, with a more rapid recent decline of 4.3% between 1987 and 1994. **Figure 3** shows how an apparently fairly stable annual cycle of large amplitude (**Figure 3A**) reveals a distinct downward trend of area (**Figure 3B**) when anomalies from interannual monthly means are considered. (**Figure 3C**) shows that the downward trend occurs for every season of the year; the estimated mean annual loss of ice area is $(34\,300 \pm 3700)$ km^2.

The steady hemispheric decline in sea ice extent masks more violent regional changes. In the Bering Sea there was a sudden downward shift of sea ice area in 1976, indicating a regime shift in the wind stress field as the Aleutian Low moved its position. In the Arctic Basin a passive microwave analysis of the length of the ice-covered season during 1979–86 showed a see-saw effect, with amelioration in the Russian Arctic, Greenland, Barents, and Okhotsk Seas and a worsening in the Labrador Sea, Hudson Bay, and the Beaufort Sea. A further analysis extended the coverage to 1978–96 and confirmed these results: the Kara/Barents Sea region had the highest rate of decline in area, of 10.5% per decade, followed by the seas of Okhotsk and Japan and the central Arctic Basin at 9.7 and 8.7% respectively. Lesser declines were experienced by the Greenland Sea (4.5%), Hudson Bay (1.4%), and the Canadian Arctic Archipelago (0.6%). Increases were registered

in the Bering Sea (1% – the starting date being later than the 1976 collapse), Gulf of St Lawrence (2%), and Baffin Bay/Labrador Sea (3.1%). Taking the more modern data into account it is clear that the see-saw effect discovered over 1979–86 has been largely subsumed into a general retreat.

A particularly important area of sea ice retreat has been the central part of the Greenland Sea gyre, in the vicinity of 75°N 0–5°W. This is normally the site of strong wintertime convection, driven by salt fluxes from local ice growth over the cold Jan Mayen Current, which produces the tongue-like Odden feature. Cold off-ice winds move newly formed ice eastward within the tongue so that the net salt flux in the western part of the feature is strongly positive; this is where convection occurs. Tracer experiments have shown that deep convection has failed to reach the bottom since about 1971 and in recent years has been greatly reduced in volume and confined to the uppermost 1000 m, while ice production has also been reduced, with no Odden forming at all in 1994, 1995, and 2000. The salt flux produces the causal link between ice retreat and convection shut-off.

What is the reason for these changes? Climatic simulations by GCMs predict that the global warming effect due to increased atmospheric CO_2 should be amplified in the polar regions, particularly the Arctic, mainly through the ice–albedo feedback effect. However, a more immediate cause of many of the observed changes can be identified as a changed pattern of atmospheric circulation in high latitudes. In the North Atlantic sector of the Northern Hemisphere this can be represented by the North Atlantic Oscillation (NAO) index, the wintertime difference in pressure between Iceland and Portugal, which was low or negative through most of the 1950s–1970s but has been rising since the 1980s and which has been highly positive throughout the current decade. A high positive NAO index is associated with an anomalous low pressure center over Iceland which involves enhanced west and north-west winds over the Labrador Sea (cold winds which cause increased cooling hence increased convection), enhanced east winds over the Greenland Sea in the 72–75° latitude range (causing a reduction in local ice growth in the Odden ice tongue, and a reduced separation between growth and decay regions, hence a reduced rate of convection); enhanced north-east winds in the Fram Strait area, causing an increased area flux of ice through the Strait (although the ice may have a reduced thickness, so the volume flux is not necessarily increased); and an enhanced wind-driven flow of the North Atlantic Current, allowing more warm water to enter the Atlantic layer of the Arctic Ocean.

Within the Arctic Basin this pattern is incorporated into a large-scale wintertime pattern (with associated index) called the Arctic Oscillation (AO), which involves a see-saw of sea level pressure (SLP) between the Arctic Basin and the surrounding zonal ring. The anomaly appears to extend into the upper atmosphere, and so represents an oscillation in the strength of the whole polar vortex. **Figure 4** shows the results of an analysis of the differences in SLP over the Arctic Ocean between high and low NAO years (corresponding also to different phases of the AO index). What had been thought of as the Arctic 'norm', i.e. a high over the Beaufort Sea leading to the familiar Beaufort Gyre and Trans Polar Drift Stream as the resulting free drift (along the isobars) ice circulation pattern, is actually the result of a low NAO (situation B). With a high NAO (situation A) the Beaufort High is suppressed and squeezed towards the Alaskan coast, causing a reduction in the area and strength of the Beaufort Gyre, and a tendency for ice produced on the Siberian shelves to turn east and perform a longer circuit within the basin before emerging from the Fram Strait (this applies also to the trajectory of fresh water from Siberian rivers). The weakening of the Beaufort Gyre may well explain anomalously low summer sea ice extents observed in the Beaufort Sea in 1996–98 (**Figure 5**), since locally melting ice is not replaced by new inputs of ice from the north east. The difference field (situation C) aptly demonstrates these changes if one considers the differential ice drift vectors as occurring along the isobars shown. Situations A and B represent two distinct patterns of Arctic Ocean circulation, which may be called 'cyclonic' and 'anticyclonic' respectively.

Antarctic

Seasonal variability The sea ice cover in the Antarctic is one of the most climatically important features of the Southern Hemisphere. Its enormous seasonal variation in extent greatly outstrips that of Arctic sea ice, and makes it second only to Northern Hemisphere snow extent as a varying cryospheric feature on the Earth's surface. **Figure 6** shows monthly averaged sea ice extent and concentration maps for the Antarctic, derived in the same way as **Figure 1** from SMMR passive microwave data, and covering the same period, 1979–87.

With the seasons reversed, the maximum ice extent occurs in August and September. At its maximum (**Figure 6A**) the ice cover is circumpolar in extent. Moving clockwise, the ice limit reaches 55°S in the Indian Ocean sector at about 15°E, but lies at

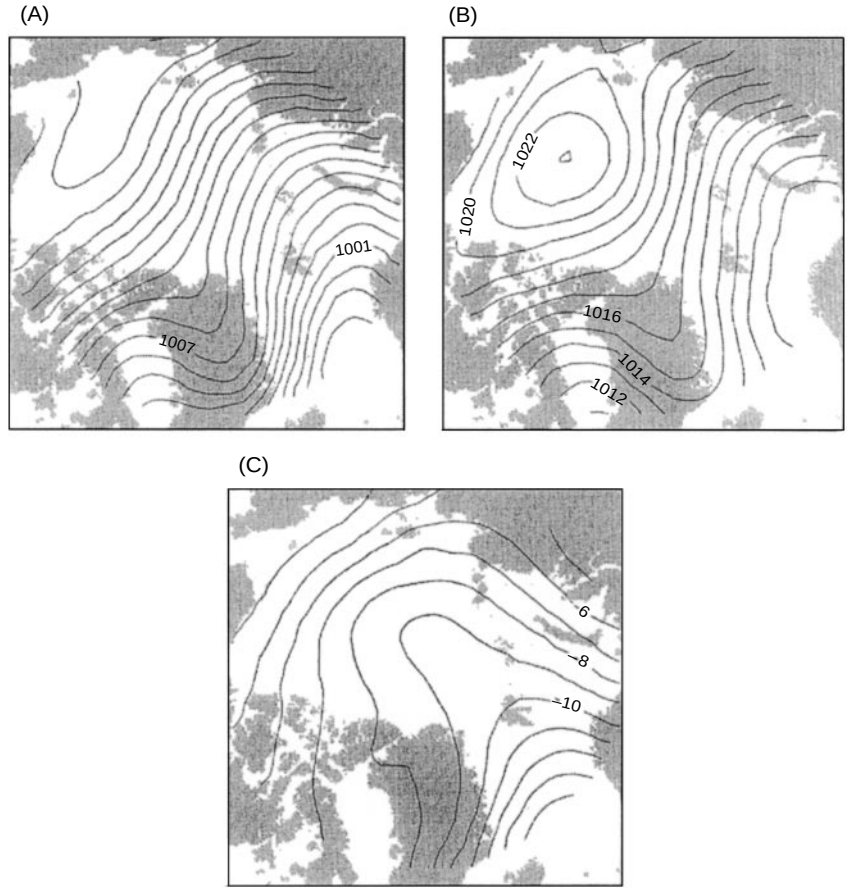

Figure 4 Pressure fields over the Arctic Ocean corresponding to (A) high North Atlantic Oscillation index, (B) low NAO index, (C) the difference field. (Reproduced with permission from Kwok and Rothrock (1999) *Journal of Geophysical Research,* 104: 5177–5189.

about 60°S around most of the rest of east Antarctica, then slips even further south to 65°S off the Ross Sea. The edge moves slightly north again to 62°S at 150°W, then again shifts southward to 66°S off the Amundsen Sea before moving north again to engulf the South Shetland and South Orkney Islands off the Antarctic Peninsula and complete the circle. The zonal variation in latitude of this winter maximum therefore amounts to some 11°. It has been found that the winter advance of the ice edge follows closely the advance of the 271.2°C isotherm in surface air temperature (freezing point of sea water) and almost coincides with this isotherm at the time of maximum advance. The ice limit is therefore mainly determined thermodynamically, with the gross zonal variations in the winter ice limit matching zonal variations in the freezing isotherm (due to the distribution of continents in the Southern Hemisphere). Smaller-scale variations in the maximum ice limit may be related to deflections in the Antarctic Circumpolar Current as it crosses submarine ridges. Note that within the ice limit the ice concentration is generally less than the almost 100% concentration found in the Arctic Ocean in winter. Even in the areas of greatest concentration, the central Weddell and Ross Seas, it is only in the range 92–96%, while there is a broad marginal ice zone facing the open Southern Ocean over which the concentration steadily diminishes over an outer band of width 200–300 km. This has been found to be a zone over which the advancing winter ice edge is composed of pancake ice, maintained as small cakes by the turbulent effect of the strong wave field.

Ice retreat begins in October and is rapid in November and December. Again the retreat is circumpolar but has interesting regional features. In the sector off Enderby Land at 0–20°E a large gulf opens up in December to join a coastal region of reduced ice concentration which opens in November. This is a much attenuated version of a winter polynya which was detected in the middle of the pack ice in this sector during 1974–76, but which has only recurred very occasionally as an open-water feature since that date, e.g. in 1994. It was

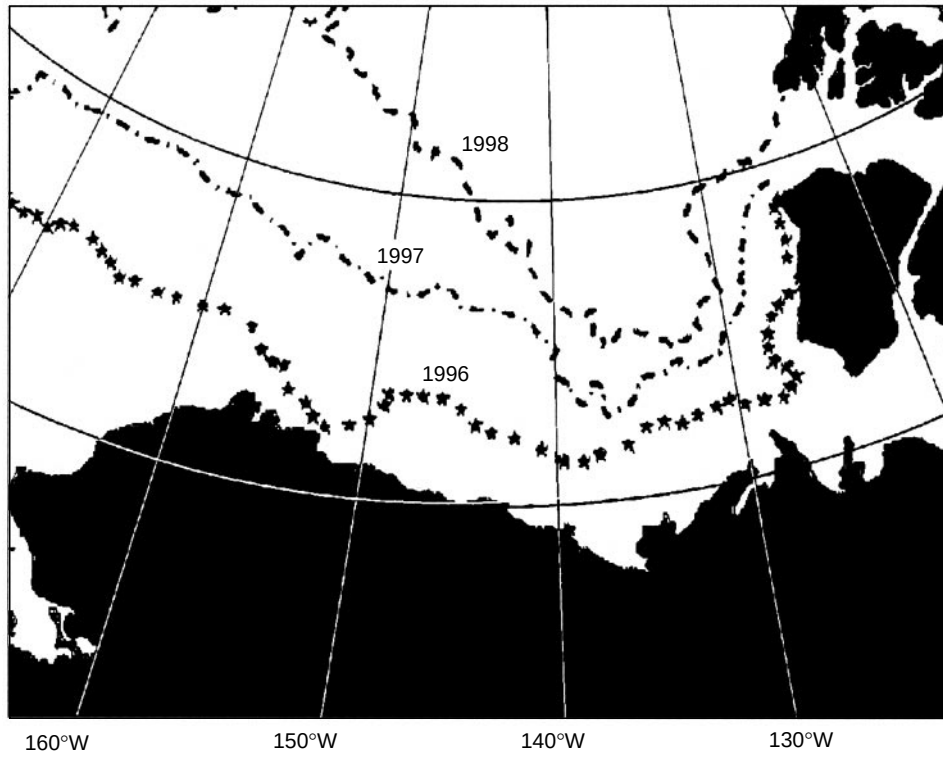

Figure 5 Beaufort Sea ice edge retreat in recent summers.

known as the Weddell Polynya and lay over the Maud Rise, a plateau of reduced water depth. The area was investigated in winter 1986 by the Winter Weddell Sea Project (WWSP) cruise of FS 'Polarstern', and it was found that the region is already part of the Antarctic Divergence, where upwelling of warmer water can occur, and that additional circulating currents and the doming of isopycnals over the rise could allow enough heat to reach the surface to keep the region ice-free in winter. Since the occurrence is irregular, the region is presumably balanced on the edge of instability. The 1986 winter cover was of high concentration but was very thin. The December distribution also shows an open-water region appearing in the Ross Sea, the so-called Ross Sea Polynya, with ice still present to the north. In November and December a series of small coastal polynyas can be seen to be actively opening along the east Antarctica coast.

By January (**Figure 6B**) further retreat has occurred. The Ross Sea is now completely open, east Antarctica has only a narrow fringe of ice around it, and large ice expanses are confined to the eastern Ross Sea, the Amundsen-Bellingshausen Sea sector (60–140°W), and the western half of the Weddell Sea. The month of furthest retreat is February. Ice remains in these three regions, but most of the east Antarctic coastline is almost ice-free, as is the tip of the Antarctic Peninsula. This is the season when supply ships can reach Antarctic bases, when tourist ships visit Antarctica, and when most oceanographic research cruises are carried out. It can be seen that the ice concentration in the center of the western Weddell Sea massif is still 92–96%. This is the region which bears the most resemblance to the central Arctic Ocean; it is the only part of the Antarctic to contain significant amounts of multi-year ice, it is very difficult to navigate, and consequently even its bathymetry is not as well known as that of other parts of the Antarctic Ocean.

By March the very short Antarctic summer is over and ice advance begins. The first advances take place within the Ross and Weddell Seas, then circumpolar advance begins in April. During May and June the Weddell Sea ice swells out to the north east, while around the whole of Antarctica the ice edge continues to advance until the August peak.

Figure 7 is the Antarctic equivalent of **Figure 2**. The annual cycle of ice extent can be seen to have a much higher amplitude than in the Arctic, and the year-to-year variability of the peaks and troughs is also somewhat greater. During the 8.8-year record, the February average extent varies from 3.4 to $4.3 \times 10^6\,\mathrm{km}^2$, while the September average extent

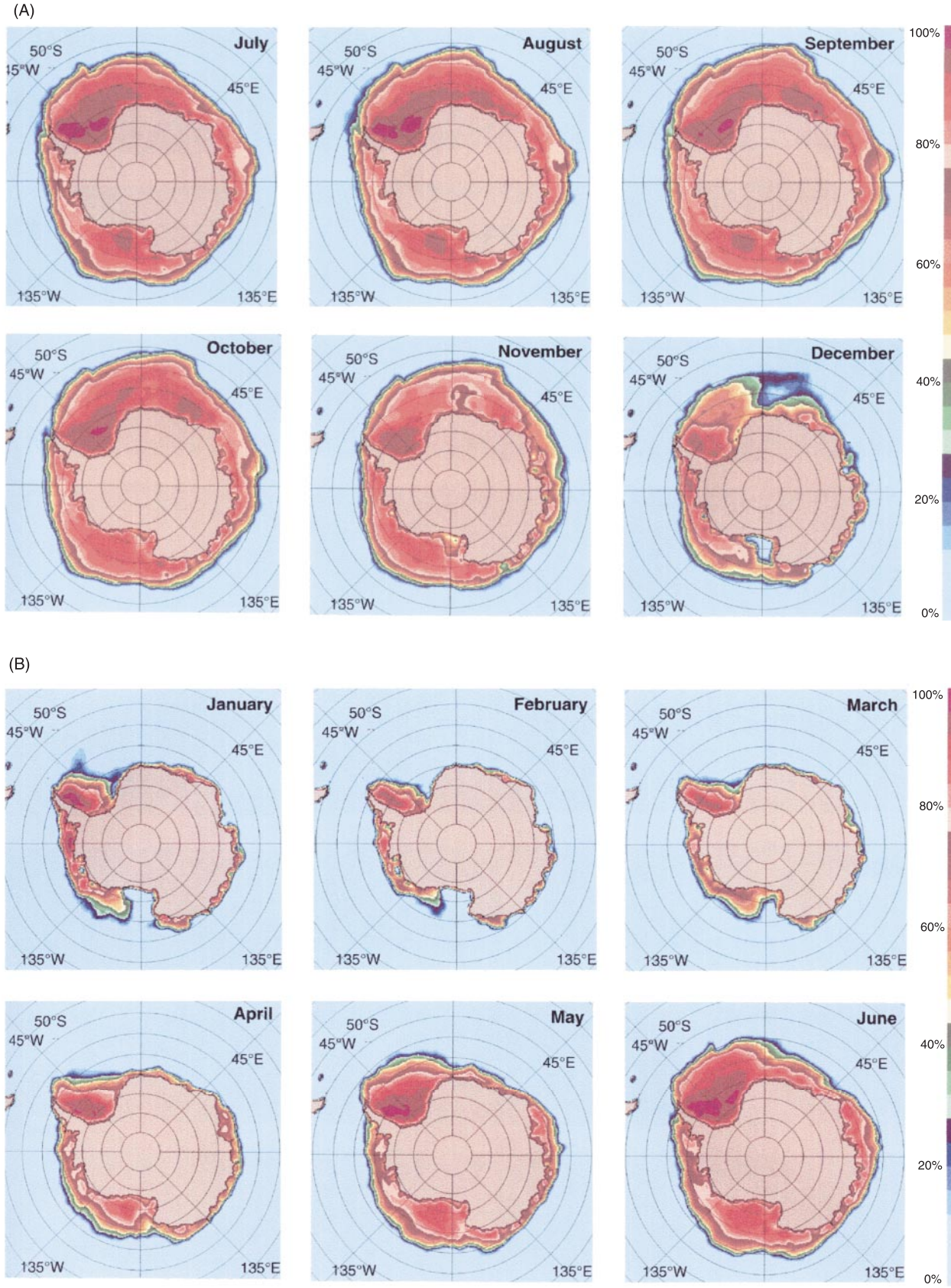

Figure 6 Sea ice extent and concentration maps for the Antarctic for (A) winter, (B) summer months, from SMMR passive microwave data averaged over the period 1979–87. (Reproduced with permission from Gloersen *et al.*, 1992.)

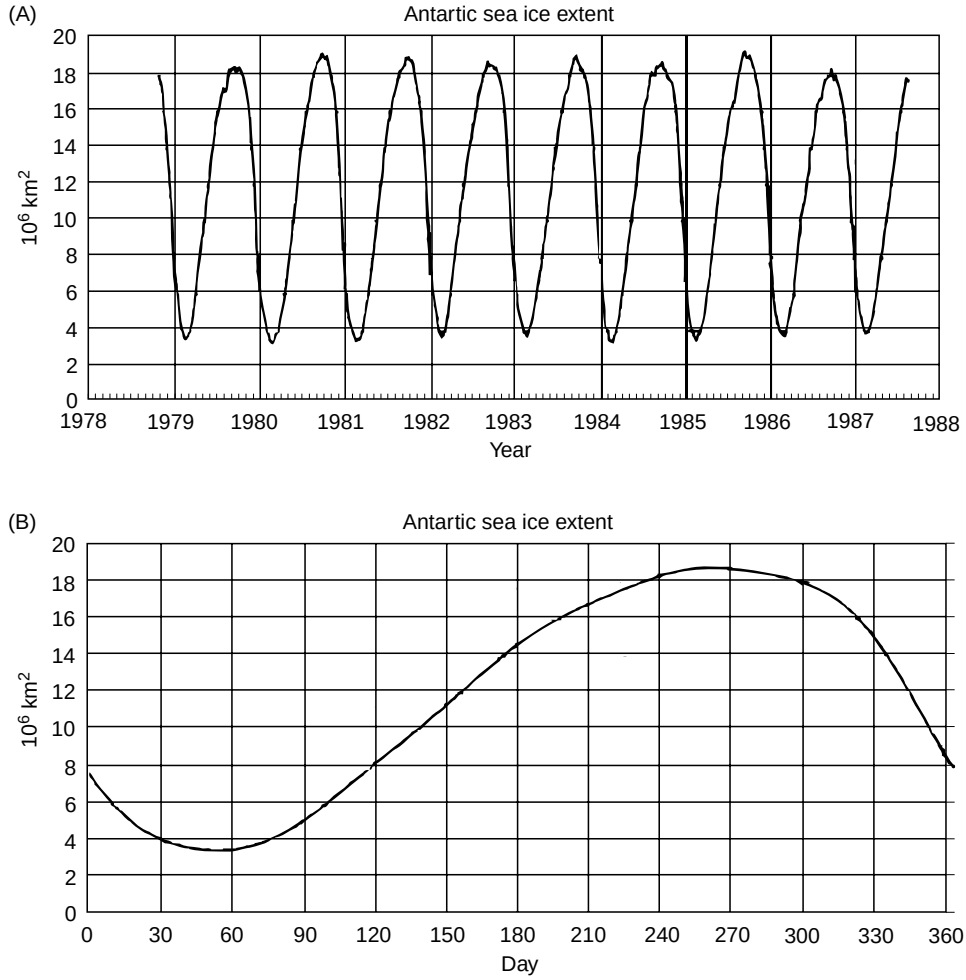

Figure 7 (A) The cycle of Antarctic sea ice extent for the 1979–87 period; (B) the averaged seasonal cycle. (Reproduced with permission from Gloersen *et al.*, 1992.)

varies from 15.5 to $19.1 \times 10^6\,\text{km}^2$, both covering ranges of $\pm$ 10–12%. The overall average cycle (**Figure 7b**) shows a retreat which is steeper than the advance. The mean minimum extent, at the end of February, is $3.6 \times 10^6\,\text{km}^2$, while the mean maximum extent, in the middle of September, is $18.8 \times 10^6\,\text{km}^2$. Because of low average ice concentrations within the pack, the corresponding minimum and maximum ice areas are 2.1 and $15.0 \times 10^6\,\text{km}^2$.

The winter ice extent in the Antarctic exceeds that of the Arctic winter, while the summer minima are very much lower. This implies that the combined Arctic and Antarctic sea ice extent should be greatest during the Arctic summer. **Figure 8** shows that in fact the peak occurs in October after a plateau during the summer and that the global minimum occurs in late February. The range is approximately $19–29 \times 10^6\,\text{km}^2$, with a high interannual variability for both maxima and minima.

Interannual variability Observational data on Antarctic sea ice extent show no significant trend. Passive microwave data for the 1988–94 period show no evidence of an overall trend in extent, but some evidence suggesting that anomaly patterns propagate eastward, offering support for the idea of an Antarctic circumpolar wave in surface pressure, wind, temperature, and sea ice extent. During the 7 years of the study, ice seasons shortened in the east Ross Sea, Amundsen Sea, west Weddell Sea, offshore eastern Weddell Sea, and east Antarctica between 40° and 80°E. Ice seasons lengthened in the west Ross Sea, Bellingshausen Sea, central Weddell Sea, and the region 80°E–135°E. Earlier evidence of a major ice retreat in the Bellingshausen Sea in the summer of 1988–91 was shown to be a short-lived phenomenon. A longer-term statistical analysis of passive microwave data from 1978 onwards gave a small and not statistically significant upward trend in overall Antarctic ice extent, of some 1.3% per

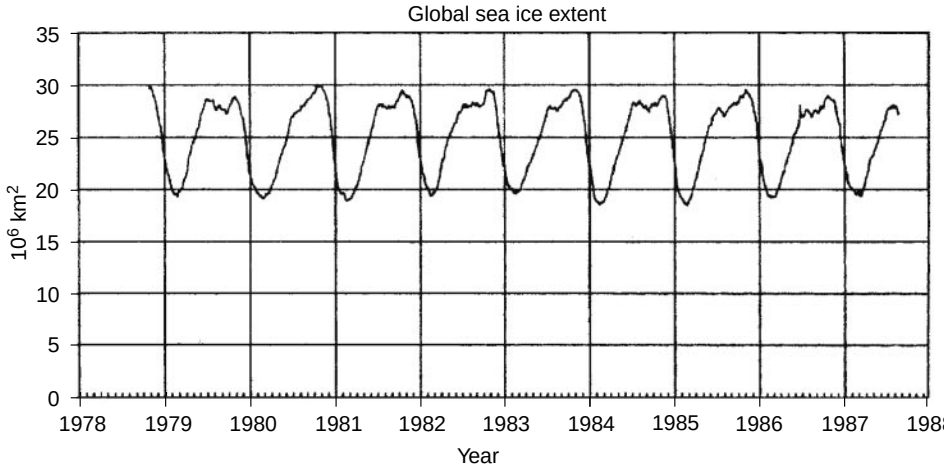

Figure 8 Combined global cycle of sea ice extent, 1979–87 (Reproduced with permission from Gloersen *et al.*, 1992.)

decade. The conclusion is that sea ice extent and GCM predictions agree in showing no strong trend.

Sea Ice Thickness

Arctic

Knowledge of the regional and temporal variability of ice thickness in the Arctic comes mainly from upward sonar profiling by submarines. Therefore the level of knowledge depends on whether submarines have been able to operate in the area concerned. Until now, data have been obtained mainly from British submarines operating in the Greenland Sea and Eurasian Basin since 1971, and from US submarines operating in the Canada and Eurasian Basins since 1958.

Results show that the ice in Baffin Bay is largely thin first-year ice with a modal thickness of 0.5–1.5 m. In the southern Greenland Sea too, the ice, although composed largely of partly melted multiyear ice, also has a modal thickness of about 1 m, with the decline in mean thickness from Fram Strait giving a measure of the freshwater input to the Greenland Sea at different latitudes. Over the Arctic Basin itself there is a gradation in mean ice thickness from the Soviet Arctic, across the Pole and towards the coasts of north Greenland and the Canadian Arctic Archipelago, where the highest mean thicknesses of some 7–8 m are observed. These overall variations are in accord with the predictions of numerical models which take account of ice dynamics and deformation as well as ice thermodynamics. The overall basin mean is about 5 m in winter and 4 m in summer.

In order to assess whether significant changes are occurring in a region of the Arctic it is necessary to obtain area-averaged observations of mean ice thickness over the same region using the same equipment at different seasons or in different years. Ideally the region should be as large as possible, to allow assessment of whether changes are basin-wide or simply regional. Also the measurements should be repeated annually in order to distinguish between a fluctuation and a trend. Because of the unsystematic nature of Arctic submarine deployments this goal has not yet been achieved, but a number of comparisons have been carried out which strongly suggest that a significant thinning has been occurring. Some of these have been made possible by very large new datasets which have been obtained from the US SCICEX civilian submarine program during 1993–99.

SCICEX data obtained in September–October of 1993, 1996, and 1997 have been compared with data obtained during six summer cruises during the period 1958–76. Twenty-nine crossing places were identified, where a submarine track from the recent period crossed one from the early period, and the corresponding tracks (of average length 160 km) were compared in thickness. In each case the mean thicknesses obtained were adjusted to a standard date of September 15 using an ice–ocean model to account for seasonal variability. The 29 matched datasets were divided into six geographical regions (**Figure 9**). The decline in mean ice draft was significant for every region and increased across the Arctic from the Canada Basin towards Europe – it was 0.9 m in the Chukchi Cap and Beaufort Sea, 1.3 m in the Canada Basin, 1.4 m near the North Pole, 1.7 m in the Nansen Basin, and 1.8 m in the eastern

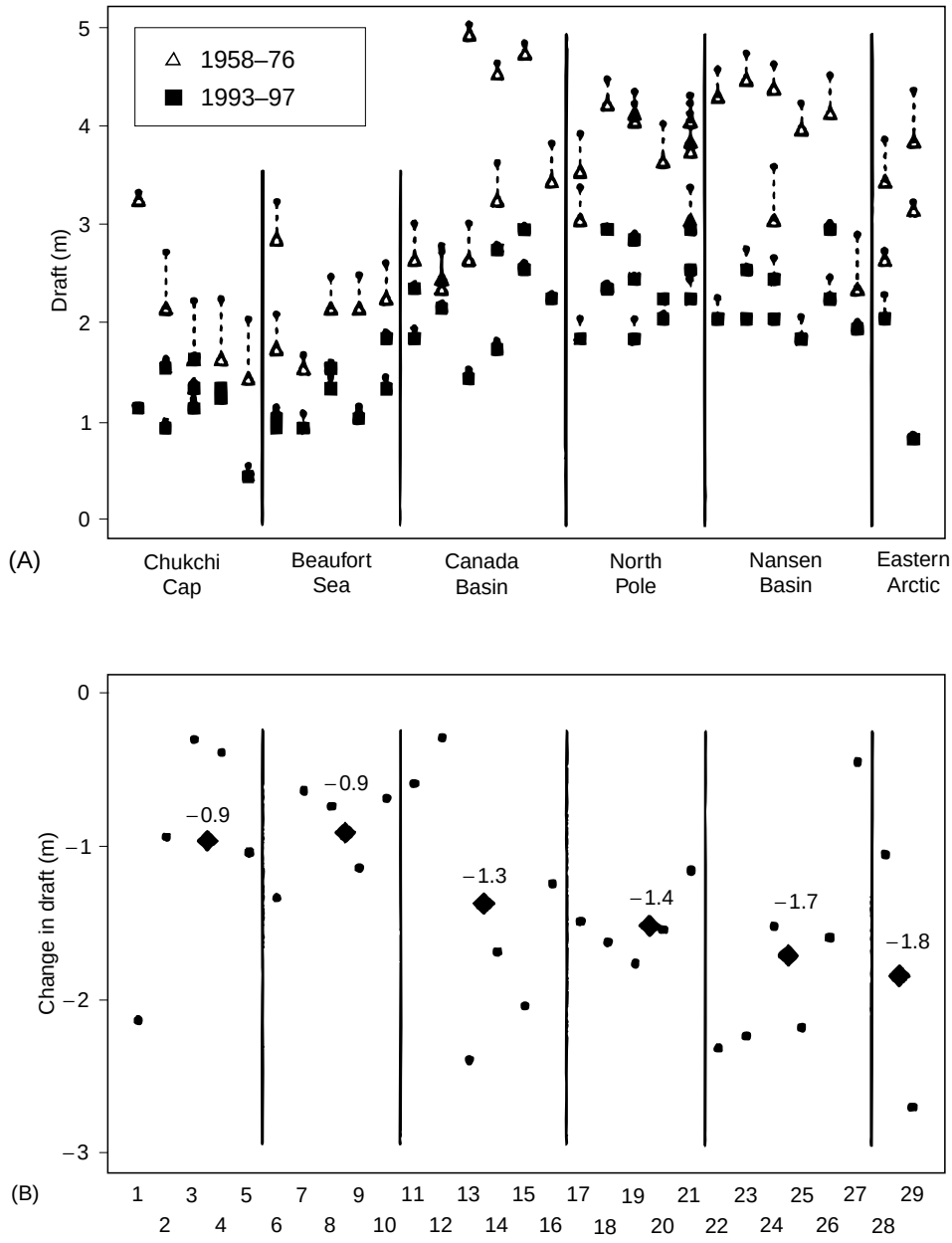

Figure 9 (A) Mean ice drafts at crossings of early cruises with cruises in the 1990s. Early data (1958–76) are shown by open triangles and those from the 1990s by solid squares, both seasonally adjusted to September 15. The small dots show the original data before the seasonal adjustment. The crossings are grouped into six regions separated by the solid lines and named appropriately. (B) Changes in mean ice draft at cruise crossings (dots) from the early data to the 1990s. The change in the mean ice draft for all crossings in each region is shown by a large diamond. (Reproduced with permission from Rothrock *et al.* (1999) *Geophysical Research Letters* (1999) 26: 3469–3472.)

Arctic. Overall, the mean change in draft was from 3.1 m in the early period to 1.8 m in the recent period, a decline of 42%.

The authors of the study commented that the decline in mean draft could arise thermodynamically from any of the following flux increases:

1. A $4\,W\,m^{-2}$ increase in ocean heat flux,
2. A $13\,W\,m^{-2}$ increase in poleward atmospheric heat transport, or
3. A $23\,W\,m^{-2}$ increase in downwelling shortwave radiation during summer.

Clearly a change in ice dynamics can also produce a change in mean ice draft, although it is not known what change in wind forcing would be needed to

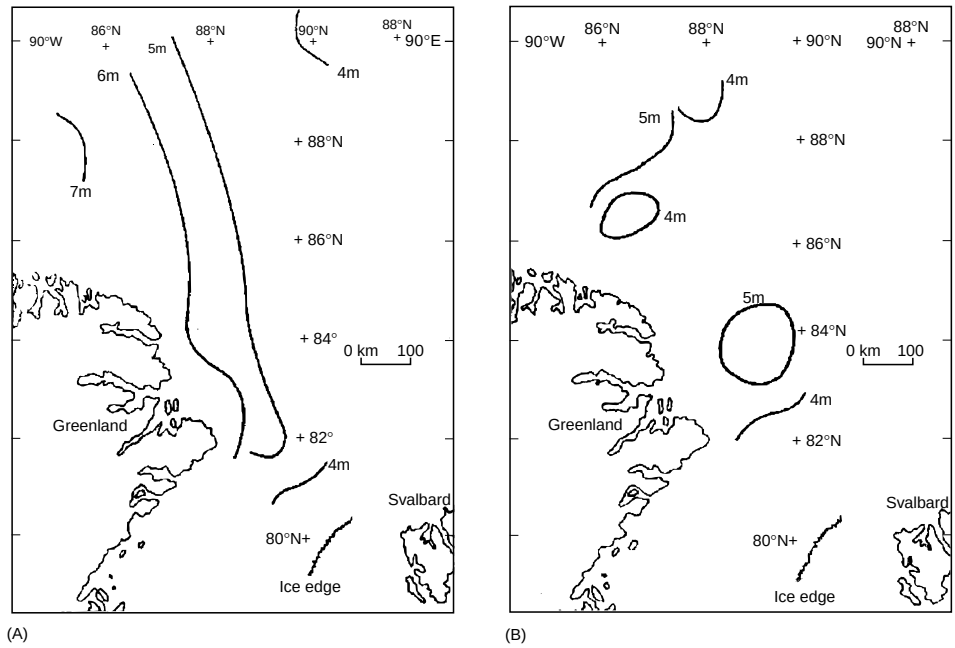

Figure 10 Contour maps of mean ice drafts from the Eurasian Basin measured from British submarines, October 1976 and May 1987. (Reproduced with permission from Wadhams (1990) *Nature* 345: 795–797.)

account for the magnitude and distribution of the observed draft decrease.

This is the most extensive comparison so far, but it should be noted that all datasets involved are from summer, mostly late summer, so that the reported decline refers to only one season of the year, and that most track comparisons occur over the North Pole region and Canada Basin, with few in the Eurasian Arctic and none south of 84° in the Eurasian Basin.

Complementary to this study are comparisons from the Eurasian Basin and Greenland Sea made using data from British submarine cruises. One comparison (**Figure 10**) involved datasets from a triangular region extending from Fram Strait and the north of Greenland to the North Pole, recorded in October 1976 and May 1987. Mean drafts were computed over 50 km sections, and each value was positioned at the centroid of the section concerned; the results were contoured to give the maps shown in **Figure 10**. There was a decrease of 15% in mean draft averaged over the whole area (300 000 km^2), from 5.34 m in 1976 to 4.55 m in 1987. Profiles along individual matching track lines showed that the decrease was concentrated in the region south of 88°N and between 30° and 50°W. By comparison of the entire shape of the probability density functions of ice draft, the conclusion was that the main contribution to the loss of volume was the replacement of multiyear and ridged ice by young and first-year ice. For instance, taking ice of 2–5 m thickness as an indicator of undeformed multiyear ice fraction, this declined from 47.6% in 1976 to 39.1% in 1987, a relative decline of 18%. This is in agreement with a recent finding that multiyear ice fraction in the Arctic (estimated from passive microwave data) suffered a 14% decrease during the period 1978–98. This multiyear ice variability correlated well with mean ice thickness variability from the eastern Arctic as estimated from surface oscillation measurements made from Russian drifting stations (note that the oscillation technique, an inference based on the peak period of swell propagating through the ice, has not been validated against direct measurements).

The British study did not correct for seasonal variability between the 1976 measurements, made in October, and those of 1987, made in April–May. If this is done using a model, the decrease in mean ice draft (standardized to September 15) becomes much greater at 42%, since April–May is the time of greatest ice thickness. This is in excellent agreement with results for the entire overall US dataset, yet occurred within a period of only 11 years. This indicates either that thinning occurs faster in the Eurasian Basin than elsewhere in the Arctic or that it is invalid to compare datasets from different times of year simply by standardizing to 'summer' through use of a model.

The latter problem is largely overcome in an analysis of the most recent British dataset, obtained in

Table 1 Mean drafts in 1° bins of latitude in 1976 and 1996

Latitude range	*Mean draft m in 1996*	*Mean draft m in 1976*	*1996 as % of 1976*
81–82	1.57	5.84	26.9
82–83	2.15	5.87	36.6
83–84	2.88	4.90	58.7
84–85	3.09	4.64	66.6
85–86	3.54	4.57	77.4
86–87	3.64	4.64	78.5
87–88	2.36	4.60	51.2
88–89	3.24	4.41	73.4
89–90	2.19	3.94	55.5
Overall	2.74	4.82	56.8

September 1996 by HMS 'Trafalgar'. These data can be compared directly with results from October 1976. The two submarines followed similar courses between 81°N and 90°N on about the 0° meridian, and it was found that about 2100 km of track from each submarine, when divided into 100 km sections, were close enough in correspondence to count as 'crossing tracks'. The overall decline in mean ice thickness between 1976 and 1996 was 43%, in remarkably close agreement with US results. The mean drafts in 1° bins of latitude were as shown in **Table 1**.

It can be seen that there was a significant decrease of mean draft at every latitude, but that the decline is largest just north of Fram Strait and near the Pole itself. A characteristic of the ice cover observed from below was the large amount of completely open water present at all latitudes. A seasonality correction to the 1976 data for the slight difference in mean draft between October and September brings the ratio to 59.0% for September, a decline of 41%. Thus the British and the US data are in remarkably good agreement in describing a very significant decrease in the thickness of Arctic Ocean sea ice.

A cautionary note must be sounded in that these significant decreases in thickness derived from spatially averaged data conceal large random variabilities at given locations. Time-series of ice draft at fixed locations have been obtained from moored upward sonar systems, of which the most comprehensive set spans Fram Strait. An analysis of data from 1991 to 1998 showed that interseasonal and interannual variability in thickness far exceed any trend, although of course the length of the dataset is only 7 years.

A possible direct cause of the observed thinning is the recent discovery that the Atlantic sublayer in the Arctic Ocean, which lies beneath the polar surface water and which derives from the North Atlantic Current, has warmed substantially (by 1–2°C at 200 m depth) and increased its range of influence relative to water of Pacific origin. The front separating the two water types has now shifted from the

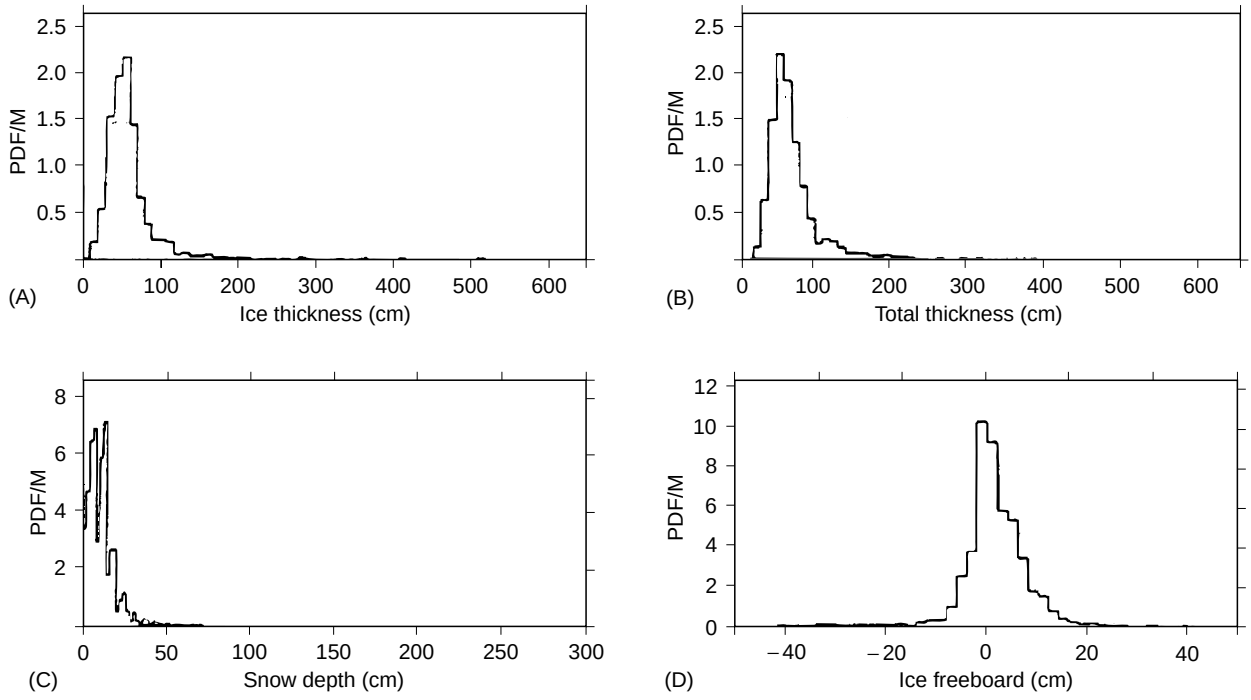

Figure 11 Thickness distributions of Antarctic first-year sea ice (A), ice plus snow (B), and snow alone (C). The distribution of ice freeboards is shown in (D); a negative value permits water infiltration. (Reproduced with permission from Wadhams *et al.* (1987) *Journal of Geophysical Research* 92: 14535–14552.)

Lomonosov to the Alpha-Mendeleyev Ridge. This warmer and shallower sublayer should increase the ocean heat flux into the bottom of the ice. This is enhanced by the fact that the structure of the polar surface layer has itself changed. In the Eurasian Basin there was formerly a cold halocline layer in the 100–200 m depth range, where temperature stayed cold with increasing depth despite salinity rising. Its existence was due to riverine input from Siberia, which has recently diverted eastward due to a changed atmospheric circulation, causing a retreat of the cold halocline and possibly associated with the recently observed summertime retreat of sea ice in the Beaufort Sea sector (**Figure 5**).

Antarctic

Knowledge of ice thickness in the Antarctic is much less extensive than in the Arctic, since systematic data have been obtained mainly by repetitive drilling except for the use of moored upward sonar at certain sites in the Weddell Sea. The winter pack ice in the Antarctic is of global importance because of its vast extent and large seasonal cycle, so the determination of winter ice thickness remains a high research priority.

In 1986 the first deep penetration into the circumpolar Antarctic pack during early winter, the time of ice edge advance, was accomplished by the WWSP cruise of FS 'Polarstern', during which systematic ice thickness measurements (at 1 m intervals along lines of about 100 holes) were made throughout the eastern part of the Weddell-Enderby Basin, from the ice edge to the coast, covering Maud Rise and representing a typical cross-section of the first-year circumpolar Antarctic pack during the season of advance. After a spring cruise in 1988 a second winter cruise was carried out in 1989: the Winter Weddell Gyre Study (WWGS) involved a crossing of the Weddell Sea from the tip of the Antarctic Peninsula to Kap Norvegia in the east during September–October, and thus allowed the multiyear ice regime of the western Weddell Sea to be studied in midwinter.

In the advancing Antarctic pack, composed of first-year consolidated pancake ice, the ice thickness distribution was as shown in **Figure 11**. Note the

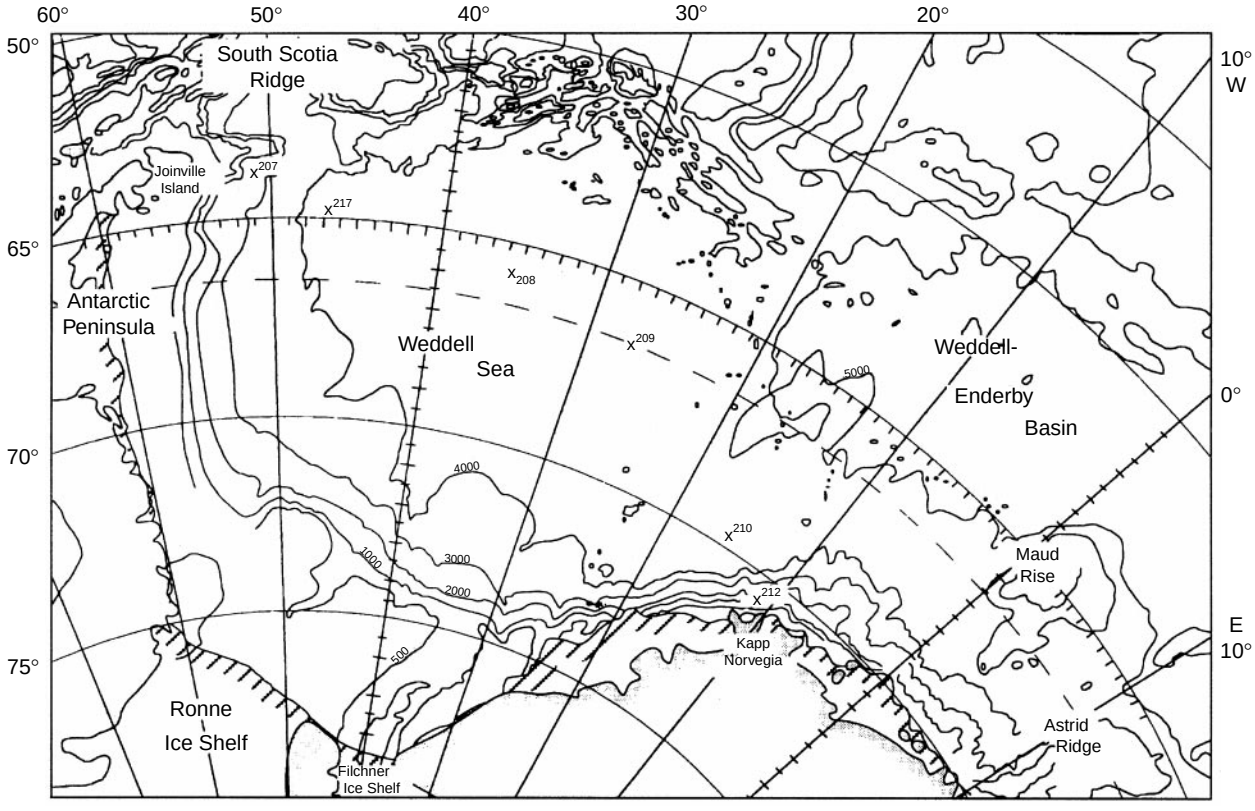

(A)

Figure 12 (A) Locations of six moored upward-looking echo sounders in the Weddell Sea. (B) Mean ice drafts December 1990–December 1992 from these sounders. (Reproduced with permission from Jeffries, 1998.)

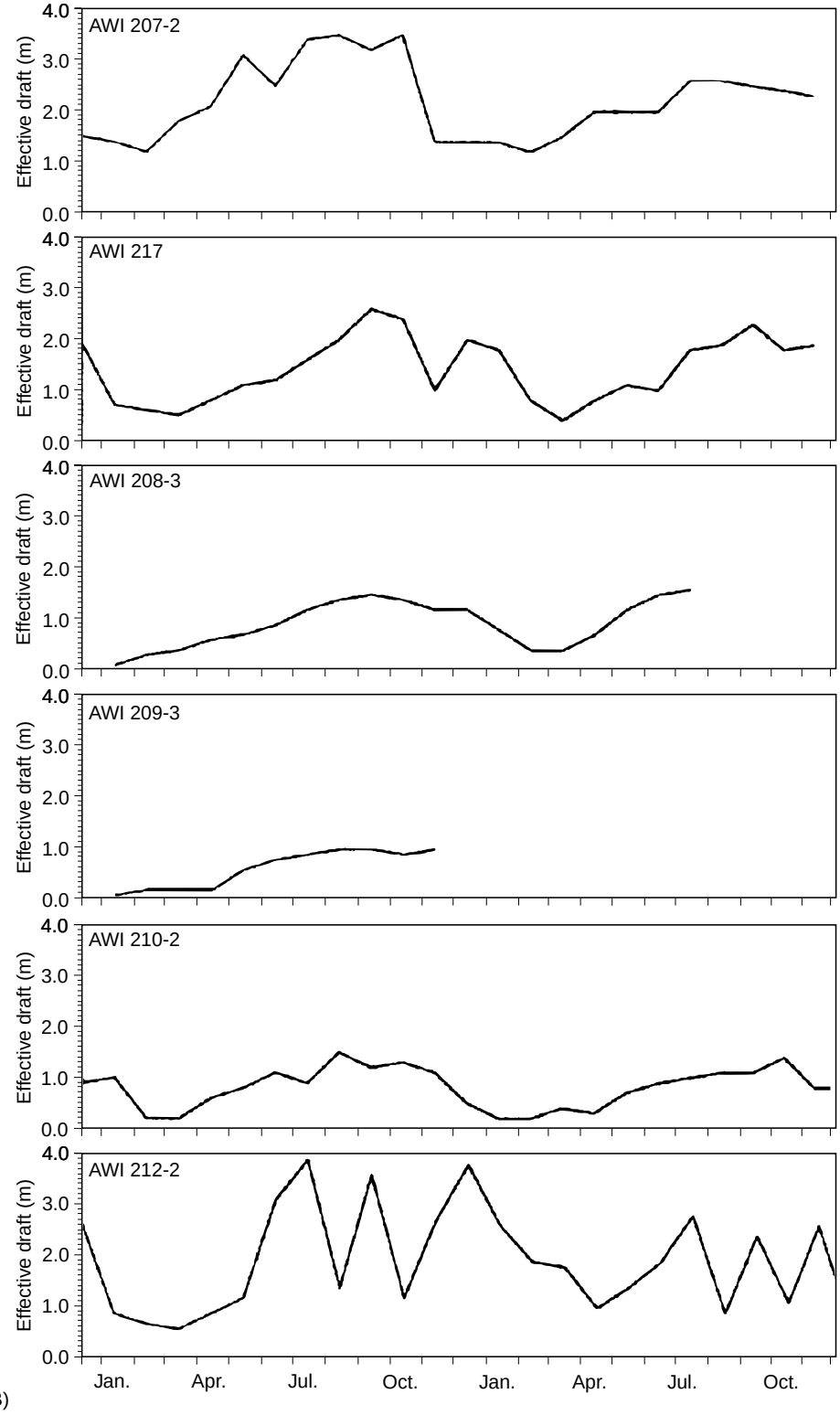

(B)

Figure 12 *Continued*

peak at the very low value of 50–60 cm, with a peak in snow cover thickness at 14–16 cm. The snow cover was sufficient to push the ice surface below water level in some 17% of holes drilled, and this leads to water infiltration into the snow layer and the formation of a new type of ice, snow-ice, at the

boundary between ice and overlying snow. It is reasonable to suppose that the pancake ice-forming mechanism is typical of the entire circumpolar advancing ice edge in winter (neglecting embayments such as the Ross and Weddell Seas).

Multiyear ice was measured in 1989 in the western Weddell Sea; the Weddell Gyre carries ice from the eastern Weddell Sea deep into high southern latitudes in the southern Weddell Sea off the Filchner-Ronne Ice Shelf, and then northward up the eastern side of the Peninsula to the north-west Weddell Sea. This journey takes about 18 months, and so permits much of the ice to mature into multiyear (strictly, second-year) ice. Multiyear ice can be identified by its structure in cores, and by the very thick snow cover which it acquires, which is almost always sufficient to depress the ice surface below the waterline. Ice drilling showed that the mean thickness of undeformed multiyear ice (1.17 m), was about double that of first-year ice (0.60 m). The presence of ridging roughly doubles the mean draft of the 100 m floe sections in which it occurs (0.60–1.03 m in first-year; 1.17–2.51 m in multiyear). In addition, snow is very much deeper on multiyear ice (0.63–0.79 m) than on first-year ice (0.16–0.23 m).

Drilling from ships has the three advantages that data can be obtained from many locations, that first-year ice and multiyear ice can be clearly discriminated, and that the detailed structure of ridges can be measured. In other respects, however, moored upward-looking echo sounders (ULES) give far more information. Data were collected from six such ULES systems moored across the Weddell Sea (**Figure 12A**) during a 2 year period from December 1990 to December 1992. The results for mean drafts (**Figure 12B**) are in good agreement with drilling data for winter, but also reveal the annual cycle ('effective draft' in this figure is true mean draft, i.e. including the open water component). It can be seen that the westernmost ULES, in the Weddell Sea outflow (207), has a cycle ranging from just over 1 m in summer to about 3 m in winter, in good agreement with ridged multiyear ice sampled from drilling. The thickness diminishes considerably over the central Weddell Sea (208, 209) but then rises again near the Enderby Land coast (212) to a very variable mean value. This last ULES, very close to the coast, is in a shear zone where much ridging can occur as well as deformation around grounded icebergs.

In summary, Antarctic sea ice of a given age is much thinner on average than Arctic sea ice, but the overlying snow cover can be thicker. The reasons for the great snow thickness in multiyear Antarctic ice are that the snow does not necessarily melt during the first summer, while during its second year it enters the inner part of the Weddell Sea where precipitation is greater. In the central Arctic snow depth may reach 40 cm by the end of the first winter, but the snow melts in summer so that snow thickness on multiyear ice is a function only of time of year. In the Antarctic the snow thickness is sufficient to push the ice–snow interface below sea level in 17% of cases sampled for first-year ice and up to 53% for second- and multiyear ice. It has been estimated that the resulting snow-ice (or so-called 'meteoric ice') makes up 16% of the ice mass in the Weddell Sea. Finally, in the Antarctic much of the ice has a fine-grained structure of randomly oriented crystals, formed from the freezing of a frazil ice suspension to form pancakes, then the freezing together of pancakes to form consolidated pancake ice, the typical first-year ice type forming in the advancing winter ice edge region. In the Arctic most ice has formed by congelation growth and so shows a crystal fabric of columnar-grained ice with horizontal c-axes. A mechanical difference is that in the Antarctic most ridges appear to be formed by buckling and crushing of the material of the floes themselves, and so are composed of a small number of fairly thick blocks extending to modest depths – typically 6 m or less. In the Arctic ridges tend to be formed by the crushing of thin ice in refrozen leads between floes, and so are composed of a large mass of small blocks, extending to greater depths – typically 10–20 m, with significant numbers extending to 30 m or more and even to 40–50 m in extreme cases.

See also

Antarctic Circumpolar Current. Arctic Basin Circulation. Coupled Sea Ice-Ocean Models. Current Systems in the Atlantic Ocean. Current Systems in the Southern Ocean. General Circulation Models. Icebergs. Ice–Ocean Interaction. Ice-shelf Stability. Polynyas. Sea Ice: Overview. Weddell Sea Circulation.

Further Reading

Ackley SF and Weeks WF (eds). (1990). *Sea Ice Properties and Processes*, CRREL Monograph 90-1. Hanover, NH: US Army Cold Regions Research and Engineering Laboratory.

Gloersen P, Campbell WJ, Cavalieri DJ *et al.* (1992) *Arctic and Antarctic Sea Ice, 1978–1987: Satellite Passive-microwave Observations and Analysis*. National Aeronautics and Space Administration, Report NASA SP-511.

Jeffries MO (ed.) (1998) *Antarctic Sea Ice: Physical Processes, Interactions and Variability,* Antarctic

Research Series 74. Washington: American Geophysical Union.
Leppäranta M (ed.) (1998) *Physics of Ice-Covered Seas*, vols 1 and 2. University of Helsinki Press.
Wadhams P (2000) *Ice in the Ocean*. London: Gordon and Breach.
Wadhams P, Dowdeswell JA and Schofield AN (eds) (1996) *The Arctic and Environmental Change*. London: Gordon and Breach Publishers.
Wadhams P, Gascard J-C and Miller L (eds) (1999) The European Subpolar Ocean Programme: ESOP. *Deep-Sea Research II* 46: 1011–1530 (special issue).
Wheeler PA (ed.) (1997) 1994 Arctic Ocean Section. *Deep-Sea Research II* 44: (Special issue)
Zwally HJ, Comiso JC, Parkinson CL *et al.* (1983). *Antarctic Sea Ice 1973–1976: Satellite Passive Microwave Observations*. Washington, DC: NASA, Report. SP-459.

SEA LEVEL CHANGE

J. A. Church, Antarctic CRC and CSIRO Marine Research, Tasmania, Australia
J. M. Gregory, Hadley Centre, Berkshire, UK

doi:10.1006/rwos.2001.0268

Introduction

Sea-level changes on a wide range of time and space scales. Here we consider changes in mean sea level, that is, sea level averaged over a sufficient period of time to remove fluctuations associated with surface waves, tides, and individual storm surge events. We focus principally on changes in sea level over the last hundred years or so and on how it might change over the next one hundred years. However, to understand these changes we need to consider what has happened since the last glacial maximum 20 000 years ago. We also consider the longer-term implications of changes in the earth's climate arising from changes in atmospheric greenhouse gas concentrations.

Changes in mean sea level can be measured with respect to the nearby land (relative sea level) or a fixed reference frame. Relative sea level, which changes as either the height of the ocean surface or the height of the land changes, can be measured by a coastal tide gauge.

The world ocean, which has an average depth of about 3800 m, contains over 97% of the earth's water. The Antarctic ice sheet, the Greenland ice sheet, and the hundred thousand nonpolar glaciers/ice caps, presently contain water sufficient to raise sea level by 61 m, 7 m, and 0.5 m respectively if they were entirely melted. Ground water stored shallower than 4000 m depth is equivalent to about 25 m (12 m stored shallower than 750 m) of sea-level change. Lakes and rivers hold the equivalent of less than 1 m, while the atmosphere accounts for only about 0.04 m.

On the time-scales of millions of years, continental drift and sedimentation change the volume of the ocean basins, and hence affect sea level. A major influence is the volume of mid-ocean ridges, which is related to the arrangement of the continental plates and the rate of sea floor spreading.

Sea level also changes when mass is exchanged between any of the terrestrial, ice, or atmospheric reservoirs and the ocean. During glacial times (ice ages), water is removed from the ocean and stored in large ice sheets in high-latitude regions. Variations in the surface loading of the earth's crust by water and ice change the shape of the earth as a result of the elastic response of the lithosphere and viscous flow of material in the earth's mantle and thus change the level of the land and relative sea level. These changes in the distribution of mass alter the gravitational field of the earth, thus changing sea level. Relative sea level can also be affected by local tectonic activities as well as by the land sinking when ground water is extracted or sedimentation increases. Sea water density is a function of temperature. As a result, sea level will change if the ocean's temperature varies (as a result of thermal expansion) without any change in mass.

Sea-Level Changes Since the Last Glacial Maximum

On timescales of thousands to hundreds of thousands of years, the most important processes affecting sea level are those associated with the growth and decay of the ice sheets through glacial–interglacial cycles. These are also relevant to current and future sea-level rise because they are the cause of ongoing land movements (as a result of changing surface loads and the resultant small changes in the shape of the earth – postglacial rebound) and ongoing changes in the ice sheets.

Sea-level variations during a glacial cycle exceed 100 m in amplitude, with rates of up to tens of millimetres per year during periods of rapid decay of the ice sheets (**Figure 1**). At the last glacial